NANO LETTERS

2007
Vol. 7, No. 9
2638−2641

$Sn_{78}Ge_{22}$@Carbon Core–Shell Nanowires as Fast and High-Capacity Lithium Storage Media

Hyojin Lee and Jaephil Cho*

Department of Applied Chemistry, Kumoh National Institute of Technology, Gumi, 730-701 Korea

Received May 1, 2007; Revised Manuscript Received June 5, 2007

ABSTRACT

Branched $Sn_{78}Ge_{22}$@carbon core–shell nanowires were prepared by thermal annealing of butyl-capped $Sn_{78}Ge_{22}$ clusters at 600 °C in a vacuum. The first discharge and charge capacities are 1250 and 1107 mA h/g, showing a Coulombic efficiency of 88%. Such a one-dimensional core–shell design exploits the benefits of the $Sn_{78}Ge_{22}$ nanowire to produce an exceptional high rate lithium reactivity (93% Coulombic efficiency at 8C (=6400 mA/g) rate) as well as excellent capacity retention after extended cycles (capacity retention of 94%).

One of the most intensively studied anode materials for lithium batteries is Sn due to its relatively high theoretical capacity (991 mA h/g) and high electronic conductivities ($\sim 10^4$ s/cm) compared to other lithium reactive metals.[1] In contrast to the metal hosts, lithium alloys Li_xM possess a highly ionic character and, thus, are usually very brittle. Mechanical stresses related to volume changes in excess of 200% induce pulverization and aggregation as well as loss of the electrical interphase contact.[2] Although such a drastic volume change cannot be removed completely, the degree of the volume change can be reduced. In this regard, two methods have been proposed. The first involves forming an alloy with a ductile active metal so that it acts as a buffer for volume expansion.[3] The second method is similar to the first: bulk- or nanosized metals are coated with carbon or are dispersed in the carbon matrix.[4,5] Here, carbon and inactive conducting metal medium act as an electrical connector with the Cu current collector when the particles pulverized. These methods utilize zero-dimensional bulk particles or nanoparticles.

Syntheses and electrochemical studies of one-dimensional lithium reactive metal nanowires are rarely reported, and Si nanowires prepared by a laser ablation method have shown a reversible capacity <500 mA h/g.[6] General synthetic methods for preparing metallic nanowires use vapor−liquid−solid (VLS),[7,8] solution−liquid−solid (SLS) or vapor−solid (VS) reactions.[9,10]

In this study, $Sn_{78}Ge_{22}$@carbon core−shell nanowires are produced by the thermal annealing of the butyl-capped $Sn_{78}Ge_{24}$ particles connected to each other as a wire. The nanowires have diameters in the range of 50−100 nm, lengths of several micrometers, and are crystalline as grown. Electrochemical Li dealloy/alloy results show that the nanowires test at 93% capacity retention at the 8C rate (=6400 mA/g). They also show a first charge capacity of 1107 mA h/g.

Our simple synthetic approach uses clusters of the butyl-capped $Sn_{78}Ge_{22}$ nanoparticles, and vacuum annealing of these clusters tuned into $Sn_{78}Ge_{22}$@carbon core−shell nanowires (Figure 1a). Figure 1b exhibits a transmission electron microscopy (TEM) image of butyl-capped $Sn_{78}Ge_{22}$ nanoparticles before annealing. With these nanoparticles, particles 1 μm in size are connected to each other. The electron diffraction (inset of b) pattern confirms the formation of the amorphous phase. Typically, Ge[11] or $Sn_{0.9}Si_{0.1}$[12] nanoparticles obtained from similar synthetic methods are of a similar particle size while the particles are unconnected. Furthermore, the particles in the image consist of clusters of nanosized particles ($\sim$5−10 nm) capped with butyl groups. Hence, a similar occurrence can be expected with the sample before annealing. After the sample was thermal annealed at 600 °C in a vacuum, the morphology before annealing changed completely, showing branched nanowires with diameters in a range of 50−100 nm and lengths that were several micrometers. As $Sn_{78}Ge_{22}$ particles before annealing consist of many nanoparticles capped with butyl groups, these particles can be grown in different directions when the butyl groups are burnt out, as shown in Figure 1c. A more detailed mechanism of the nanowire formation during annealing is underway. Inductively coupled plasma mass spectroscopy (ICP-MS) of the nanowires after annealing confirmed the formation of $Sn_{77}Ge_{23}$, and the carbon content determined by a CHS analyzer in the nanowires was 5 wt %. Figure 1d

* Corresponding author. jpcho@kumoh.ac.kr.

10.1021/nl071022n CCC: $37.00
Published on Web 07/28/2007

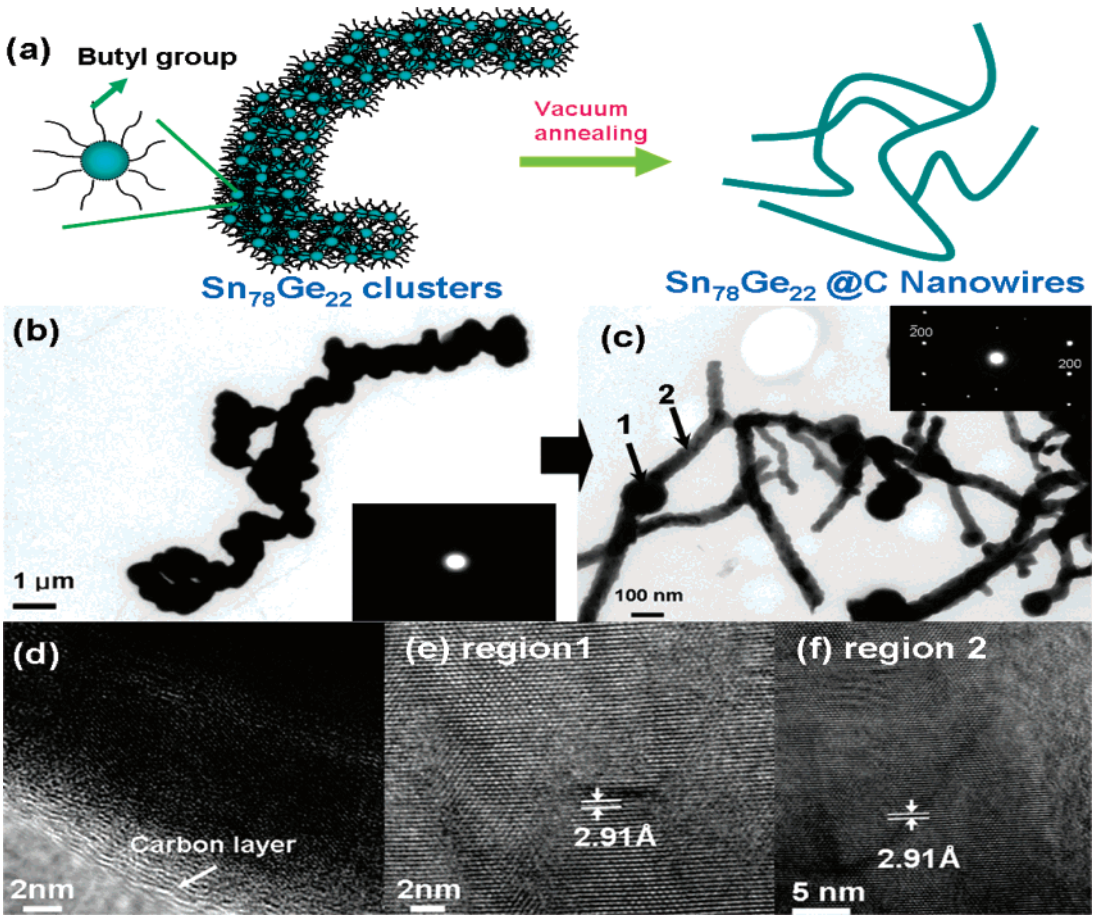

Figure 1. (a) Schematic diagram for $Sn_{78}Ge_{22}$@carbon nanowire growth from clusters of butyl-capped $Sn_{78}Ge_{22}$ nanoparticles and TEM images of the $Sn_{78}Ge_{22}$@carbon nanowires (b) before thermal annealing and (c) after thermal annealing. Insets are electron diffraction patterns of (b) and (c). (d) TEM images of region 1 in (c). (e, f) High-resolution TEM images of regions 1 and 2 in (c).

is an expanded TEM image of region 2, in which an amorphous carbon layer with a thickness of ~2 nm is shown. This carbon layer was formed from the decomposition of C_4H_9- groups during annealing. Panels e and f of Figure 1 are high-resolution images of regions 1 and 2, respectively; both images show the (200) lattice fringe corresponding to tetragonal Sn 2.98 Å. In the phase diagram of the Sn and Ge alloys, formations of other solid solution phases are not formed throughout the compositional range.[13]

A powder XRD pattern of annealed SnGe nanowires shows the formation of β-Sn with lattice constants of $a = 5.832$ and $c = 3.183$ (Supporting Information). In order to investigate the ordering degree of amorphous carbon, Raman scattering of the annealed $Ge_{78}Sn_{22}$ nanowire was performed (Figure 2a) and the dimensional ratio of the D and G band was estimated, as the ratio of D/G and was found to be 2.13. The two peaks at ~1360 and ~1580 cm^{-1} are assigned to the (disordered band) D band and (graphene band) G band, respectively.[14] This is far larger than well-ordered graphite at 0.09.[6] This result implies the formation of amorphous carbon. Figure 2b shows the Fourier transform infrared (FT-IR) spectra of butyl-capped $Sn_{87}Ge_{22}$ particles before and after annealing at 600 °C. The three peaks at 2955, 2924, and 2853 cm^{-1} fall where expected for C−H stretches of butyl groups, which is in good agreement with the results of an earlier study.[15] The peaks at 1376 and 1456 cm^{-1} are

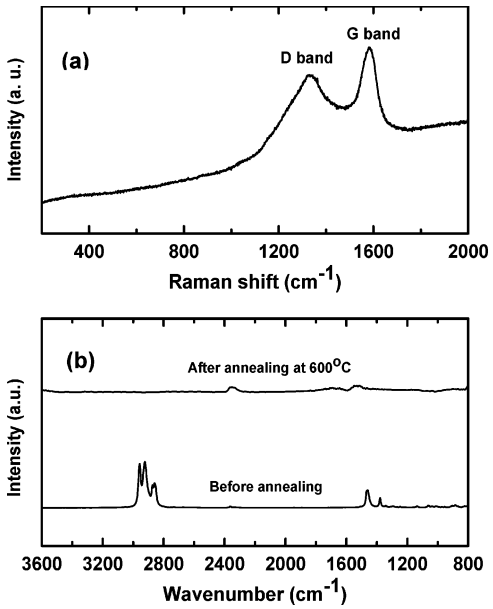

Figure 2. Raman scattering of the $Sn_{78}Ge_{22}$@carbon nanowires after thermal analysis and FT-IR spectra of $Sn_{78}Ge_{22}$@carbon nanowires before and after thermal annealing.

the positions expected for the symmetric and asymmetric bends of the butyl group, respectively.[14] The nanowire annealed at 600 °C for 5 h showed no traces of butyl groups,

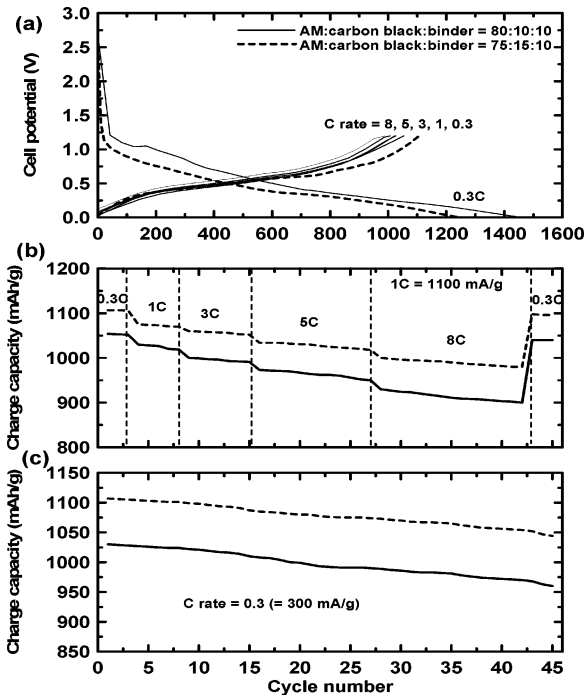

Figure 3. (a) Rate capabilities of $Sn_{78}Ge_{22}$@carbon nanowires at different C rates from 0.3, 1, 3, 5, 8C (1C = 800 mA/g) in a coin-type half cell with different electrode compositions. Discharge rate was fixed at 0.3 C. (b) Plot of rate capabilities as a function of charge capacity during extended cycling. (c) Plot of cycle number as a function of the charge capacity of $Sn_{78}Ge_{22}$@carbon nanowires.

indicating complete transformation into amorphous carbon. Typically, oxidized SnO_2 or GeO_2 is observed between 800 and 750 cm^{-1}; these are attributed to metal−O stretch.[14] In this case, no peaks in the range were observed, indicating no oxygen contamination.

Figure 3 shows the rate capabilities of the coin-type half cells with two different electrode compositions at different C rates from 0.3C to 1, 3, 6, and 8C rates (the discharge rate was fixed at 0.3C). The electrode consisted of either 75:15:10 (wt %) or 80:10:10 (wt %) (nanowire active material:carbon black:binder). In the case of 80:10:10 (wt %), the first discharge and charge capacities are 1450 and 1054 mA h/g, respectively, showing a Coulombic efficiency of 72%. However, when the electrode composition was optimized at 75:15:10 (wt %), the discharge and charge capacities show 1247 and 1107 mA h/g, respectively, corresponding to Coulombic efficiency of 88%. This value is an improved value compared to previous capped Sn[5] or Ge[16] nanoparticles that were measured below 85%. Moreover, such a Coulombic efficiency was superior to that of Si nanowires that shows the Coulombic efficiency below 50%.[6] The capacity retentions of the cells with electrode compositions of 75:15:10 (wt %) and 80:10:10 (wt %) after 45 cycles were similar to each other, showing 94 and 91%, respectively. Figure 4 shows d*Q*/d*V* curves of the nanowire for the first cycle; the increased degree of peak broadening can be observed, as compared with bulk Ge and Sn. This indicates the reduced formation of larger clusters of Sn or Ge atoms (O1 to O3). In addition, only Li_xSn peaks can be observed during lithium alloy and dealloy reactions in the

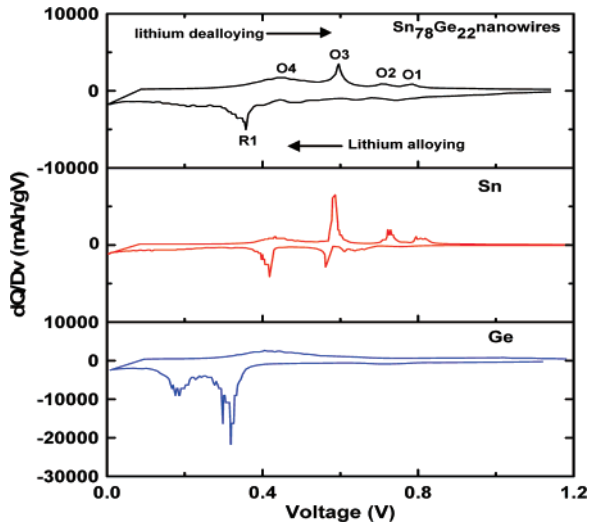

Figure 4. The differential capacity curves of $Sn_{78}Ge_{22}$@carbon nanowires (reconstructed from the voltage profile for the first cycle) of Sn and Ge.

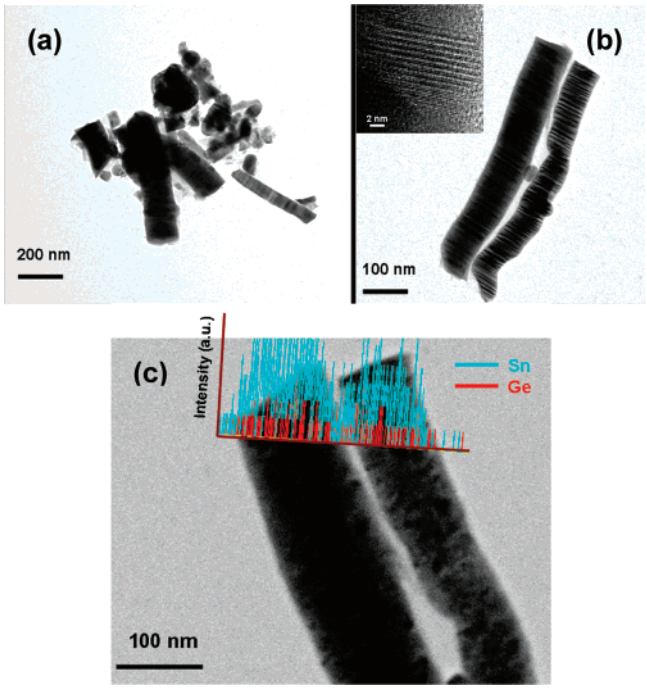

Figure 5. (a, b) TEM images of $Sn_{78}Ge_{22}$@carbon nanowires after the rate capability test in Figure 4b (inset is a high-resolution TEM image of b). (c) The EDS (energy dispersive spectroscopy) line scan across the particle.

absence of Li_xGe peaks, indicating that Ge atoms were not segregated from the alloy during cycling. However, the disappearance of the peak at ~0.6 V was observed, but the other peak positions are relatively similar to Sn, as they were between O4 and O1. The disappearance of the peak at ~0.6 V was also observed in carbon-coated Sn nanoparticles.[5b]

Figure 3b shows that charge capacities at 1, 3, 6, and 8C were 1054, 1030, 1000, and 973 mA h/g with a capacity retention at 8C of 88% in coin-type half cells containing a electrode consisting of 80:10:10 (wt %). When the electrode composition was optimized at 75:15:10 (wt %), the charge capacities at the same condition to above were improved to

1107, 1075, 1060, and 1034 mA h/g with a capacity retention at 8C of 93%.

Thus far, very few studies have reported a high-rate stability of nanoalloy particles. The excellent rate capability of the core−shell nanowires is attributed to the increased electrolyte contact area and the reduced lithium diffusion length that facilitates further Li reactions with the nanowire. For the 0D particles, repetitive particle aggregation and pulverization lead to the formation of a new surface, thus forming a new SEI (solid electrolyte interface) layer. Accordingly, part of the active metal becomes isolated by surface films formed on the fresh active surface by reactions with Li-metal compounds and electrolytes, resulting in rapid capacity fading.[17] However, due to the nature of the nanowire/carbon with the branched morphology and carbon cell, direct contact among the nanotubes can be minimized and less aggregation is expected. After the rate capability test of the nanowire/carbon nanowire was finished, a morphology change of the nanowire/carbon core−shell occurred. As shown in Figure 5a, the original branched nanowires were separated from the nanoparticles and nanowire. Furthermore, the separated nanowire has stacking faults, and microtwins are visible with their fault plane (101) plane parallel to the axis of the nanowire (Figure 5b). These defects are not observed in the pristine nanowires, and may be associated with continuous volume change during the lithium dealloy/alloy process. However, respective Sn and Ge atom segregation was not observed during cycling, as evidenced by the line mapping of Sn and Ge in the nanowires (Figure 5c).

In conclusion, branched $Sn_{78}Ge_{22}$@carbon core−shell nanowires were prepared by thermal annealing of butyl-capped $Sn_{78}Ge_{22}$ particles at 600 °C in a vacuum. Due to its morphology and carbon shell layer, the nanowires did not aggregate into larger particles but instead fragmented into nanoparticles and nanowires. The reversible capacity of the nanowire showed 1107 mA h/g, and the capacity retention after 45 cycles was 94%. Furthermore, it showed excellent capacity retention at 8C, with a capacity retention ratio of 93%.

Acknowledgment. This research was financially supported by the Ministry of Commerce, Industry and Energy (MOCIE) and Korea Industrial Technology Foundation (KOTEF) through the Human Resource Training Project for Regional Innovation. Also, financial support from University ITRC project is greatly acknowledged.

Supporting Information Available: Experimental details and XRD pattern and SEM image/EDX of the $Sn_{78}Ge_{22}$@carbon core−shell nanowires. This material is available free of charge via the Internet at http://pubs.acs.org.

References

(1) Nazri, G.-A.; Pistoia G. *Lithium Batteries Science and Technology*; Kluwer: Boston, 2004.
(2) Winter, M.; Besenhard, J. O. *Electrochim. Acta* **1999**, *45*, 31.
(3) (a) Shin, H. C.; Liu, M. *Adv. Funct. Mater.* **2005**, *15*, 582. (b) Xia, Y.; Sakai, T.; Fujieda.; Wada, M.; Yoshinaga, H. *J. Electrochem. Soc.* **2001**, *148*, 471. (c) Beattie, S. D.; Dahn, J. R. *J. Electrochem. Soc.* **2003**, *150*, A894. (d) Mao, O.; Dahn, J. R. *J. Electrochem. Soc.* **1999**, *146*, 414.
(4) (a) Kim, I.-S.; Blomgren, G. E.; Kumta, P. N. *Electrochem. Solid-State Lett.* **2004**, *7*, A44. (b) Wang, G. X.; Yao, J.; Liu, H. K. *Electrochem. Solid-State Lett.* **2004**, *7*, A250. (c) Lee, L. K.; Jung, Y. S.; Oh, S. M. *J. Am. Chem. Soc.* **2003**, *125*, 5652. (d) Noh, M.; Kim, Y.; Kim, M. G.; Lee, H.; Kwon, Y.; Lee, Y.; Cho, J. *Chem. Mater.* **2005**, *17*, 3320.
(5) (a) Kwon, Y.; Kim, M. G.; Kim, Y.; Lee, Y.; Cho, J. *Electrochem. Solid-State Lett.* **2006**, *9*, A34. (b) Noh, M.; Kwon, Y.; Lee, H.; Cho, J.; Kim, Y.; Kim, M. G. *Chem. Mater.* **2005**, *17*, 1926. (c) Kim, H.; Cho, J. *J. Electrochem. Soc.* **2007**, *154*, A462. (d) Kim, H.; Cho, J. *Electrochim. Acta* **2007**, *52*, 4197.
(6) Gao, B.; Sinha, S.; Fleming, L.; Zhou, O. *Adv. Mater.* **2001**, *13*, 816.
(7) Himpsel, F. J.; Jung, T.; Kirakosian, A.; Lin, J. L.; Petrovykh, D. Y.; Rausher, H.; Viernow, J. *MRS Bull.* **1999**, *24*, 20.
(8) (a) Wagner, R. S.; Ellis, W. C. *Appl. Phys. Lett.* **1964**, *4*, 89. (b) Cao, G. *Nanostructure and nanomaterials*; Imperial College Press: London, 2004.
(9) Trentler, T. J.; Kickman, K. M.; Goel, S. C.; Viano, S. M.; Gibbons, P. C.; Buhro, W. E. *Science* **1995**, *270*, 1791. (b) Trentler, T. J.; Goel, S. C.; Kickman, K. M.; Viano, A. M.; Chiang, M. Y.; Beatty, A. M.; Gibbons, P. C.; Buhro, W. E. *J. Am. Chem. Soc.* **1997**, *119*, 2172.
(10) Yang, P.; Lieber, C. M. *Science* **1996**, *273*, 1836. (b) Yang, P.; Lieber, C. M. *J. Mater. Res.* **1997**, *12*, 2981.
(11) Lee, H.; Kim, H.; Doo, S.-G.; Cho, J. *J. Electrochem. Soc.* **2007**, *154*, A343.
(12) Kwon, Y.; Kim, H.; Doo, S.-G.; Cho. J. *Chem. Mater.* **2007**, *19*, 982.
(13) Watanabe, T. *Nanoplating: Microstructure control theory of plated film and data base of plated film microstructure*; Elsevier Publishers: Amsterdam, The Netherlands, 2004.
(14) Yang, C.-S.; Li, Q.; Kauzlarich, S. M.; Phillips, B. *Chem. Mater.* **2000**, *12*, 983.
(15) Ferrai, A. C.; Roberston, *J. Phys. Chem. B* **2000**, *61*, 14095.
(16) Lee, H.; Kim, H.; Doo, S.-G. *J. Electrochem. Soc.* **2007**, *154*, A343.
(17) Aurbach, D.; Nimberger, A.; Markosky, B.; Levi, E.; Sominski, E.; Gedanken, A. *Chem. Mater.* **2002**, *14*, 4155.
(18) (a) Baldwin, R. K.; Pettigrew, K. A.; Ratai, E.; Augustine, M. P.; Kauzlarich, S. M. *Chem. Commun.* **2002**, 1822. (b) Baldwin, R. K.; Pettigrew, K. A.; Garno, J. C.; Power, P. P.; Liu, G.; Kauzlarich, S. M. *J. Am. Chem. Soc.* **2002**, *124*, 1150.

NL071022N